Spontaneous decay of a single quantum dot coupled to a metallic slot waveguide in the presence of leaky plasmonic modes

Yuntian Chen*, Niels Gregersen, Torben Roland Nielsen, Jesper Mørk and Peter Lodahl

DTU Fotonik, Department of Photonics Engineering, Ørsteds Plads, Building 343, DK- 2800 Kgs. Lyngby, Denmark

*yche@fotonik.dtu.dk

Abstract: We numerically investigate the coupling efficiency of a single self-assembled quantum dot to a metallic slot waveguide in the presence of leaky plasmonic modes. Leaky plasmonic modes refer to radiation modes with plasmonic features, resulting from the inhomogeneity of the dielectric environment in which the metallic slot waveguide is embedded. Compared to the ideal case of a homogenous dielectric environment, the coupling efficiency of an emitter to a metallic slot waveguide is significantly reduced. We attribute the reduction to the coupling to leaky plasmonic modes. By increasing the refractive index of the coating layer to minimize the impacts from the leaky plasmonic modes, we find that the coupling efficiency of the quantum dot to the single mode supported by the metallic slot waveguide can be enhanced by more than a factor 2.

© 2010 Optical Society of America

OCIS codes: (240.6680) Surface plasmons; (230.7370) Waveguides; (230.6080) Sources; (020.5580) Quantum electrodynamics.

References and links

1. A. Imamoglu, D. Awschalom, G. Burkard, D. P. DiVincenzo, D. Loss, M. Sherwin, and A. Small, "Quantum Information Processing Using Quantum Dot Spins and Cavity QED," Phys. Rev. Lett. **83,** 4204–4027 (1999).
2. A. V. Akimov , A. Mukherjee, C. L. Yu, D. E. Chang, A. S. Zibrov, P. R. Hemmer, H. Park, and M. D. Lukin "Generation of single optical plasmons in metallic nanowires coupled to quantum dots," Nature (London) **450**, 402–406 (2007).
3. D. E. Chang, A. S. Sørensen, P. R. Hemmer, and M. D. Lukin, "Quantum Optics with Surface Plasmons," Phys. Rev. Lett. **97**, 053002–053005 (2006).
4. G. Veronis and S. Fan, "Guided subwavelength plasmonic mode supported by a slot in a thin metal film," Opt. Lett. **30**, 3359–3361 (2005).
5. T. Ishikawa, S. Kohmoto, and K. Asakawa, "Site control of self-organized InAs dots on GaAs substrates by in situ electron-beam lithography and molecular-beam epitaxy," Appl. Phys. Lett. **73**, 1712 (1998).
6. X. Luo and T. Ishihara, "Surface plasmon resonant interference nanolithography technique," Appl. Phys. Lett. **84**, 4780 (2004).
7. J. Johansen, S. Stobbe, I. S. Nikolaev, T. Lund-Hansen, P. T. Kristensen, J. M. Hvam, W. L. Vos, and P. Lodahl, "Size dependence of the wavefunction of self-assembled InAs quantum dots from time-resolved optical measurements," Phys. Rev. B **77**, 073303–073306 (2008).
8. T. Søndergaard and B. Tromborg, "General theory for spontaneous emission in active dielectric microstructures: Example of a fiber amplifier," Phys. Rev. A **64**, 033812–033825 (2001).
9. Y. C. Jun, R. D. Kekatpure, J. S. White, and M. L. Brongersma, "Nonresonant enhancement of spontaneous emission in metal-dielectric-metal plasmon waveguide structures," Phys. Rev. B **78**, 153111–153114 (2008).
10. C. Creatore, L. C. Andreani, M. Miritello, R. L. Savio, and F. Priolo, "Modification of erbium radiative lifetime in planar silicon slot waveguides," Appl. Phys. Lett. **94**, 103112 (2009).

11. Y. Gong, S. Yerci, R. Li , L. D. Negro, and J. Vuckovic , "Enhanced light emission from erbium doped silicon nitride in plasmonic metal-insulator-metal structures," Opt. Express **17,** 20642–20650 (2009), `http://www.opticsexpress.org/abstract.cfm?URI=oe-17-23-20642`.
12. Y. C. Jun , R. M. Briggs , H. A. Atwater, and M. L. Brongersma , "Broadband enhancement of light emission in silicon slot waveguides," Opt. Express **17,** 7479–7490 (2009), `http://www.opticsexpress.org/abstract.cfm?URI=oe-17-9-7479`.
13. Y. Chen, T. Nielsen, N. Gregersen, P. Lodahl, and J. Mørk, "Finite element modeling of spontaneous emission of a quantum emitter at nanoscale proximity to plasmonic waveguides," Phys. Rev. B **81**, 125431–125441 (2010).
14. R. Zia, M. D. Selker, and M. L. Brongersma, "Leaky and bound modes of surface plasmon waveguides," Phys. Rev. B **71**, 165431–165439 (2005).
15. L. Novotny and B. Hecht, *Principles of nano-optics,* (Cambridge University Press, 2006).
16. For the guided plasmonic mode, E_x and E_z are in the plane in which the the dipole moment of QDs dominates. However the field strength of the longitudinal component (E_z) is less than 1% of the transverse components (E_x), therefore, we only consider the X component of the electric field and the exciton dipole moment for the plasmonic emission enhancement.
17. P. Berini, "Plasmon-polariton waves guided by thin lossy metal films of finite width: Bound modes of symmetric structures," Phys. Rev. B **61**, 10484–10503 (2008).

1. Introduction

The unique properties of semiconductor quantum dots (QDs), known as artificial atoms, have attracted considerable interest in the past decades. Due to their strong carrier confinement, small size, and long coherence time, such nano scale solid-state structures are expected to have significant impact on scalable quantum computing systems [1] and non-classical light sources employed in quantum communication technology. It is thus important to develop solid-state solutions, and the semiconductor technology benefits from an existing industry and possibility of integration with other functionalities.

Whatever kind of quantum mechanical degree of freedom is used, it is always desirable to achieve a very efficient coupling between a flying photonic qubit and an atomic qubit, which might function as an interface between the quantum communication system and the quantum computation system. Recently it has been proposed and experimentally demonstrated that a single quantum emitter can be efficiently coupled to surface plasmon polaritons [2, 3]. The plasmonic enhancement of light-matter interaction provides new possibilities for developing efficient single-photon sources and for mapping a quantum dot based qubit to a photonic qubit, or vice versa. We investigate such plasmonic induced enhancement of light-matter interaction, especially the preferential emission from semiconductor QDs into a desired mode supported by a realistic plasmonic waveguide, for developing efficient single-photon sources.

The structure under examination is illustrated in Fig. 1(a), showing a single self-assembled QD coupled to lithographically fabricated metallic slot waveguides [4]. Compared with other chemically grown metallic nanowires with a distribution of length and radius, the lithographic wires mainly have two advantages: (1) the self-assembled QDs can be positioned in the plane (X-Z plane) [5], as well as along the vertical direction (Y-axis); (2) the metallic slot waveguide can be fabricated lithographically [6] with controllable sizes W, H, D, as illustrated in Fig. 1(b). Meanwhile, such structures also lead to challenges since the QD emission can be quenched at interfaces [7] thus limiting how close to the plasmonic waveguide the QDs can be positioned, and in addition any inhomogeneity due to different refractive indices of the substrate and coating material is found to reduce the coupling.

In general, QDs placed near a plasmonic waveguide are subjected to multiple decay channels, namely the radiative decay channel, the non-radiative decay channel, and the plasmonic decay channel. The corresponding decay rates are denoted by γ_{rad}, γ_{nonrad}, and γ_{pl}, respectively. One notes that due to the interference between forward and backward traveling guided plasmonic modes, the localized plasmonic resonant modes in either X or Y directions can also be excited, which could substantially contribute to spontaneous emission of the QD and subsequently scat-

ter the emission out of the structure. However, the parameters of gap structure used in the paper are away from localized plasmonic resonance conditions. In addition, the measured internal quantum efficiency for the typical QDs that we are considering are 90% according to reference [7], which can be further increased by tuning the sizes. In the present paper the internal quantum efficiency of the self-assembled QD is assumed to be 100%. Hence the resistive heating of the metallic waveguide is the only mechanism of non-radiative relaxation considered. Therefore, in our case the plasmonic decay channel is dominating over spontaneous emission (SE) from the QDs, and a larger plasmonic decay rate can be used to extract coherent single photons with less influence from dephasing process of the QDs. The SE β-factor, given as the spontaneous emission decay rate for coupling to the gap mode divided by the total decay rate, i.e., $\beta = \gamma_{pl}/(\gamma_{rad} + \gamma_{nonrad} + \gamma_{pl})$, is the figure of merit of the single-photon source efficiency, which describes the fraction of the emitted energy that is coupled to the single plasmonic mode. Therefore, it is desirable to achieve, simultaneously a high plasmonic excitation rate and a high SE β-factor in the context of developing efficient and coherent single-photon sources.

It was pointed out by Jun *et al.* [9], that the emission rate enhancement due to plasmonic mode excitation in a metallic slot waveguide with homogenous dielectric environment can reach values up to 100, when the dipole emitter is properly oriented. Dielectric slot waveguides with active materials, i.e., an Er^{3+}-doped SiO_2 thin film or erbium doped silicon nitride layer, were recently studied experimentally and theoretically [10–12]. However, the coupling efficiency to the single plasmonic mode supported by the metallic slot waveguide was not examined in detail. The present paper focuses on the coupling efficiency, i.e., the SE β-factor, of the quantum dot coupled to the single plasmonic mode with special emphasis on analyzing the impact of the inhomogeneity of the surrounding material. We calculate both the plasmonic decay rate and the total decay rate of the QD using the full 3D model detailed in Ref. [13]. Our results show that the presence of leaky modes due to the inhomogeneity fairly affects the plasmonic decay rate, while the SE β-factor is substantially reduced. We find that by decreasing the index contrast within realistic experimental bounds, the SE β-factor can be increased by more than a factor of 2.

The paper is organized as follows: In Section 2, we outline the geometry under investigation and the basic theoretical requirements for modeling spontaneous emission. In Section 3, we present the results of the SE β-factor and the plasmonic decay rate both for the homogenous and inhomogeneous cases. Finally, Section 4 concludes the paper.

2. Geometry and Theory

2.1. Geometry and mode properties

We study the metallic slot waveguide shown in Fig. 1, consisting of two gold strips ($\varepsilon_{gold} = -50 + 3.85i$), a layer of quantum dots and a GaAs substrate, at the wavelength of 1000 nm. The electrodes are covered by a coating material with refractive index n_c. The geometric parameters of the waveguide and position of the single QD are illustrated in Fig. 1(b). Throughout the paper, the origin of the coordinate system for the QDs, e.g., (X_{QDs}, Y_{QDs}), is at the very middle of the gap. The calculated effective index of the guided modes versus the width of the metallic strip (W) is shown in Fig. 2(a) with fixed values of the other parameters ($n_c = 1.5$, $H = 40$ nm, $D = 30$ nm), and indicates a cutoff value of W for the higher order modes. Hence, with the typical width and height illustrated in Fig. 2(b), 2(c), such a structure can support only two guided plasmonic modes, one with E-field concentrated in the gap (gap mode) and one with E-field concentrated at the corners outside the gap (separated mode). As shown in the inset of Fig. 2(a), the propagation length of the gap mode is around 1 μm, which only allows to use as short plasmon waveguides. More specifically, the plasmons need to be coupled to dielectric waveguides within a few hundred nano meters ($4 \sim 5$ optical cycles), to avoid excessive
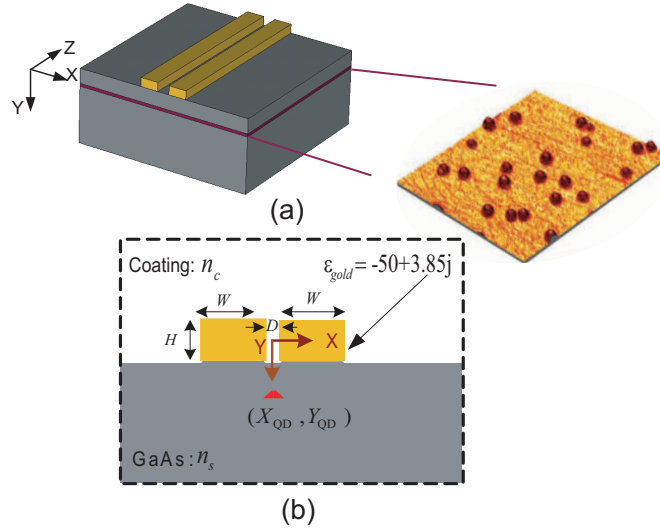
Fig. 1. (a) Sketch of QDs coupled to a metallic slot waveguide. The inserted AFM image illustrates self-assembled InAs/GaAs QDs. (b) Cross section of the metallic slot waveguide with width, height, and gap width denoted by W, H, and D, respectively.

propagation damping due to the losses of the metals.

Zia et al. [14] studied a thin Au film mounted on a fused silica substrate with air on top, which is a typical plasmonic waveguide with inhomogeneous environment examined extensively in both theory and experiment. In [14] it was found that the bounded modes are localized at the glass-Au interface, while the leaky plasmonic modes are localized at the air-Au interface. Similarly, the complete modal description of the metallic slot waveguide studied in the present paper consists of leaky modes that are characterized by effective mode indices below n_s, in addition to the gap mode and the separated mode. Depending on whether the effective mode index of these leaky modes is smaller or large than n_c, the leaky modes are entitled either radiation modes or leaky plasmonic modes in the present paper. The radiation modes can penetrate through both the substrate and the coating area and leak away, while the leaky plasmonic modes are still confined in the coating area, and can only leak away through the substrate. Due to the plasmonic features, i.e., the tight confinement of the field in the coating area as well as large field enhancement close to metals, the leaky plasmonic modes are expected to have a larger impact on the SE β-factor than the radiation modes, since the QDs are localized in the area close to the metals.

2.2. Theory

In this section we briefly outline the theoretical foundation, for further details see Refs. [8, 13]. By employing first order perturbation theory, one can use Fermi's Golden Rule [15] to calculate the decay rate of a quantum emitter,

$$\gamma = \frac{\pi \omega_0}{3\hbar\varepsilon_0} |\mu|^2 \rho_\mu(r_0, \omega_0),$$ (1)

where μ is the transition dipole moment of the quantum emitter, ρ_μ is the projected local density of states, ω_0 is the atomic transition frequency, and ε_0 is the vacuum permittivity. The projected local density of states, given by $\rho_\mu(r_0, \omega_0) = 6\omega_0[\bar{n}_\mu \cdot \text{Im}\{\bar{\bar{G}}(r_0, r_0, \omega_0)\} \cdot \bar{n}_\mu]/(\pi c^2)$, measures
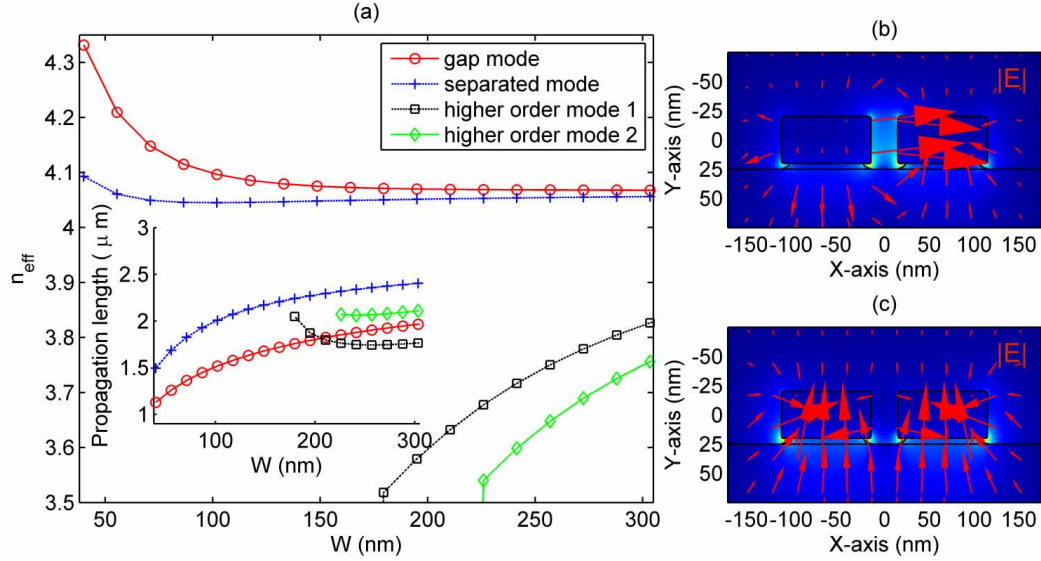
Fig. 2. (a) Effective mode index (n_{eff}) versus width of the gold strip (W) positioned on top of the GaAs substrate, with the material indices of $n_c = 1.5$, and $n_s = 3.5$. (b,c) Magnitude and orientation of the electric field in the X-Y plane for the gap mode and the separated mode for metallic waveguide with dimensions $W = 100$ nm, $D = 30nm$, $H = 40nm$. The field orientations are given by the red arrows, the length of which give the amplitude of the electric field. Inset in (a): Propagation length (field amplitude $1/e$ lengths) of the guided plasmonic modes versus W.

the available number of electromagnetic modes for a dipole located at r_0 with orientation of n_μ. The dyadic Green's function $\bar{\bar{G}}(\bar{r}, \bar{r}', \omega_0)$}, defined by $[\nabla \times \nabla \times -k_0^2 \varepsilon(\bar{r})]\bar{\bar{G}}(\bar{r}, \bar{r}', \omega_0)$} $- \bar{I}_0 \delta(\bar{r} - \bar{r}') = 0$, contains all the classical information of the electromagnetic waves and can be expanded in a set of eigenmodes. The dyadic Green's function can be split into a traverse part and a longitudinal part. Since we are studying the propagating modes, which describe the field solution in the absence of free electric charges, the longitudinal component will vanish in the following calculations. For a typical index contrast waveguide with the cladding material of ε_2, the modal description of the dyadic Green's function, more specifically the transverse part, can be formulated as follows,

$$\bar{\bar{G}}(\bar{r}, \bar{r}', \omega) = \sum_p \int_0^{+\infty} \int_{-\infty}^{+\infty} \frac{\varepsilon_2 \bar{E}_\alpha(x, y)[\bar{E}_{\tilde{\alpha}}^\dagger(x', y')]^* e^{j\beta(z-z')}}{[k_0^2 \varepsilon_2 - (\beta^2 + k_{2\perp}^2)]N_\alpha} d\beta dk_{2\perp} \qquad (2)$$

where $\bar{E}_\alpha(x, y)e^{-j(\omega_0 t - \beta z)}$ is the waveguide eigenmode labeled by α, found from the wave equation $\nabla \times \nabla \times \bar{E}(\bar{r}) - k_0^2 \varepsilon(r)\bar{E}(r) = 0$. Here, β is the longitudinal wave vector, $k_{2\perp}$ is the transverse wave vector in the cladding materials, and N_α is normalization factor defined by $N_\alpha = 2\pi \int \varepsilon(x, y)\bar{E}_\alpha(x, y) \cdot [\bar{E}_\alpha^\dagger(x, y)]^* dx dy$. Equation (2) gives the complete description of the modes, including guided modes as well as leaky modes, supported by the wave guides. For the leaky modes, β and $k_{2\perp}$ can be chosen independently, while for the guided modes β and $k_{2\perp}$ are not independent.

As can be seen from Fig. 3, there are three types of contributions to the full integration range, i.e., the gray region, the yellow region, and the poles, which represent the radiation modes, leaky plamonic modes and the guided modes, respectively. For a homogenous environment,
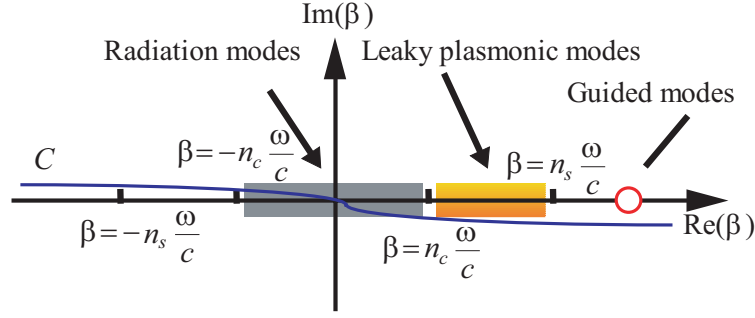
Fig. 3. Illustration of evaluating the integral representation of the dyadic Green's function. The discrete poles yield the contribution to the decay rates into the guided modes, while the gray and the yellow regions represent the continuum contributions to the radiation modes and the leaky plasmonic modes, respectively. The blue line C denotes the full integration path.

the region with leaky plasmonic modes $(n_c < \beta < n_s)$ vanishes since $n_c = n_s$. By picking up the pole contributions from the full integration range C, as illustrated in Fig. 3, one can extract the single guided mode contribution. According to our previous work [13], the normalized rate describing decay to a specific guided plasmonic mode denoted by α_0 for a QD with horizontal dipole moment is given by,

$$\frac{\gamma_{pl}}{\gamma_0} = \frac{6\pi^2 c^3 E_{\alpha_0,x}(x,y)[E^\dagger_{\alpha_0,x}(x,y)]^*}{\omega_0^2 N_\alpha \upsilon_g} \tag{3}$$

where υ_g is the group velocity, $E_{\alpha_0,x}$ denotes the x component of the electric field of the guided plasmonic mode, and γ_0 is the spontaneous emission decay rate in vacuum. The plasmonic decay rate is proportional to the field strength divided by the group velocity, which means that the emitter can release the energy to the plasmonic mode faster and more efficiently if the plasmonic mode concentrates and slows down. The total decay rate, γ_{total}, is extracted from the total power dissipation of the current source coupled to the nearby metallic waveguide from a 3D finite element model, $\gamma_{total}/\gamma_0 = P_{total}/P_0$, where $P_{total} = 1/2 \int_V \mathrm{Re}(\bar{J}^* \cdot \bar{E}_{total})dV$ is the power dissipation of the current source coupled to the metallic waveguide, and $P_0 = 1/2 \int_V \mathrm{Re}(\bar{J}^* \cdot \bar{E}_0)dV$ is the emitted power by the same current source in vacuum. Using a similar strategy, we study the length dependence of the total decay rate for the 3D finite element model to check the validity of the mode matching boundary condition that is used to absorb the gap mode, as well as the accuracy of our numerical model. We also observe the oscillations of the total decay rate due to the reflections of the radiation modes and the guided mode, as expected. Accordingly, we estimate the relative error in the calculations to be 2.5%. We refer to reference [13] for details on the implementation of the 3D finite element model.

3. Results and discussion

From Fig. 2(b), 2(c), we see that the gap mode is primarily polarized along the X axis, while the separated mode is primarily polarized along the Y axis. Therefore, for a horizontally (vertically) oriented quantum emitter, only the gap (separated) mode will be excited, while emission into the separated (gap) mode will be suppressed. Self-assembled QDs have dominating in-plane transition dipole moments. In particular, the orientation of the QD considered in the present
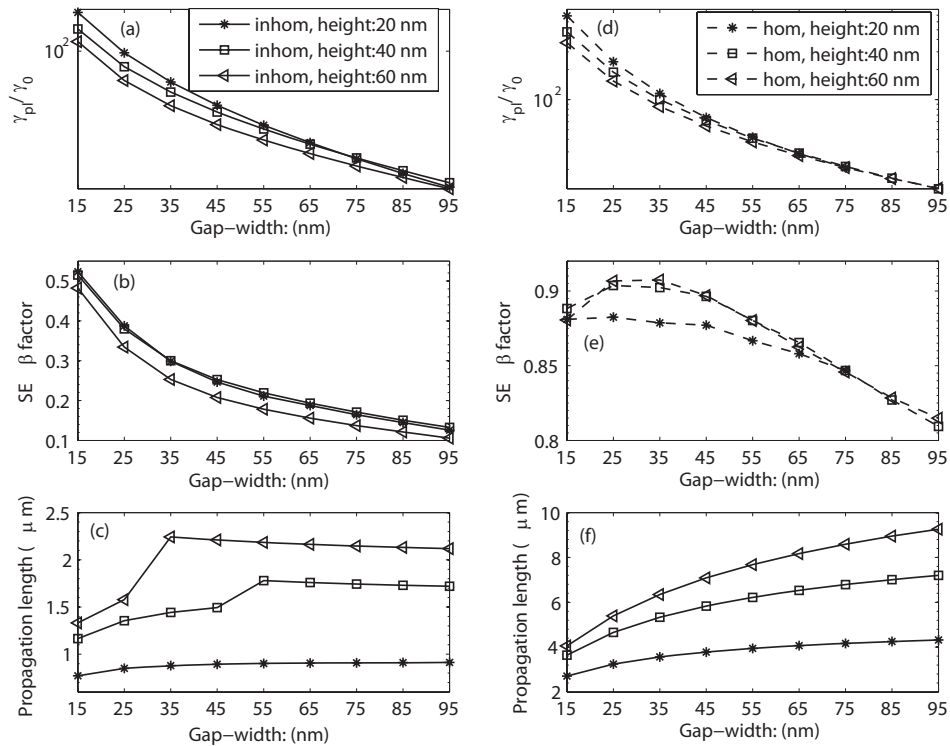
Fig. 4. Gap-width dependence of the plasmonic decay rates, SE β-factors, and the propagation length of the gap mode for an inhomogeneous dielectric environment (a, b, c) and for a homogenous dielectric environment (d, e, f). In the subplot (a, b, c), $n_c = 1.5$, $W = 100$ nm and $n_s = 3.5$, while for homogenous case in the subplot (d, e, f), the surrounding material is air ($n_{air} = 1.0$), and $W = 100$ nm.

paper is taken along X axis to achieve approximately the most efficient coupling between the QD and the gap mode [16]. Hence, light is preferentially emitted to the gap mode. We study the influence of the width of the gap, the height of the metallic strips, and the inhomogeneity on the SE β-factor for the gap mode. To avoid the field singularities induced by sharp metallic corners, the corners are smoothed by an arc with radius of 2 nm, and the substrate is etched 5 nm around the metal.

In the following calculations, the width of the metallic strip is fixed to be 100 nm to ensure operation in the regime of a single (gap) mode. First, we study gap-width dependence of the plasmonic decay rate and spontaneous emission β-factor for an ideal QD positioned in the middle of the gap ($X_{QDs} = Y_{QDs} = 0$) in Fig. 4, for both the inhomogeneous and the homogenous environment. The plasmonic decay rate for the inhomogeneous case, shown in Fig. 4(a), is comparable to that of the homogenous case, which indicates that the electric field in the middle of the gap is not much influenced by inhomogeneity, though the overall field distribution for the inhomogeneous case contracts to the substrate-coating interface. However, the SE β-factor for metallic slot waveguide embedded in an inhomogeneous dielectric environment is severely impacted by inhomogeneity. We observe three distinct features: (I) The SE β-factor
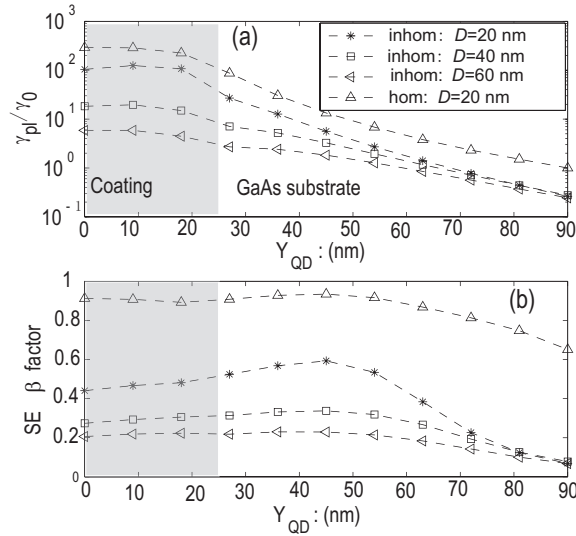
Fig. 5. Position dependence of the plasmonic decay rates and SE β-factors for the metallic slot waveguide with inhomogenous environment($n_c = 1.5$, $n_s = 3.5$) and the homogenous case ($n_c = n_s = 1.0$) with $X_{\text{QDs}} = 0$, $H = 40$ nm, $W = 100$ nm.

shown in Fig. 4(b) for the inhomogeneous case is significantly reduced compared with the homogenous case shown in Fig. 4(e); (II) In Fig. 4(b), the SE β-factor decreases monotonically with the gap-width, while for the homogenous case Fig. 4(d) indicates a maximum value of the SE β-factor for an optimized gap width when $H = 40nm$ and $H = 60nm$. We attribute such a significant reduction of the SE β-factor in Fig. 4(b) to the leaky plasmonic modes, arising from the inhomogeneity of the dielectric environment. It is well known that the interaction of light with inhomogeneities induces evanescent waves. When the metallic slot waveguide is embedded in an inhomogeneous dielectric environment, apart from the three channels mentioned in Sec. I, the evanescent waves induced by inhomogeneity of the dielectric environment will present additional competing channels for the QD, which dissipate a considerable fraction of the emitted power from the source. Secondly, the optimum gap width in Fig. 4(e) stems from the compromise of competition between the plasmonic decay channel and the non-radiative decay channel, both of which depend on the distance from the emitter to the edge of the metals. For the optimized gap width, we observe an SE β-factor larger than 90%, which indicates that with 90% success probability a single optical plasmon will be generated, and consequently can be employed as an efficient single-photon source.

From a waveguiding point of view, there is a tradeoff between the confinement of the optical field and the propagation length [17], since the more confined the field of the mode is, the shorter the mode propagates due to the intrinsic losses of the metals. In order to couple the optical plasmons out as single photons, the optical plasmons are required to propagate with a reasonable distance, i.e., a few micro meters. From Fig. 4(f), we can see clearly the tradeoff between the plasmonic excitation rate and the propagation lengths, since the plasmonic excitation rate is proportional to the confinement of the field. In the inhomogeneous dielectric environment, shown in Fig. 4(c), the tradeoff between the plasmonic excitation rates and the propagation lengths can also be observed for small gap widths, while for larger gaps, the field distribution depends more and more on the dielectric inhomogeneity, which means that the propagation length does not increase any further, although the field is less confined. Apart from
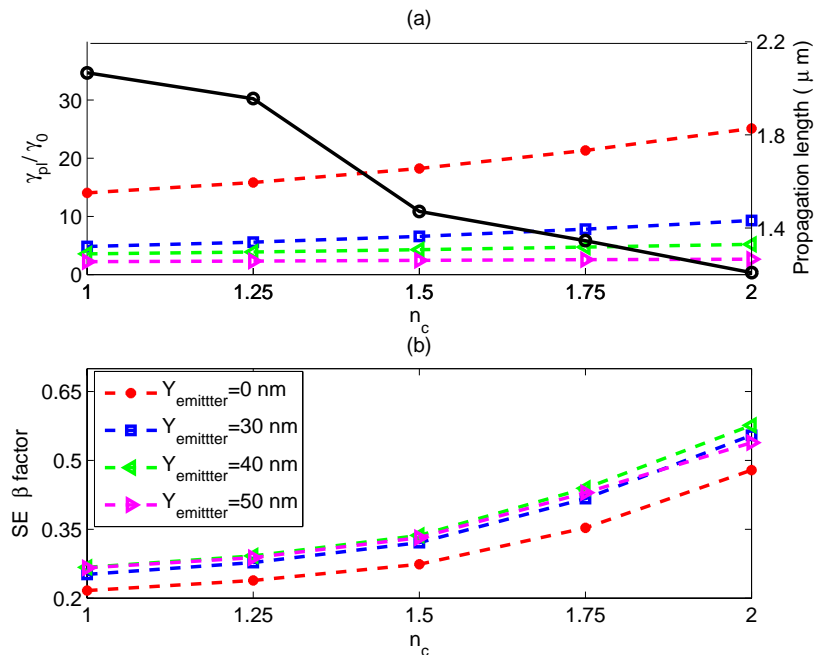
Fig. 6. Role of inhomogeneous environment, quantified by variation of plasmonic decay rate and SE β-factor with n_c for fixed $n_s = 3.5$, $X_{QDs} = 0$, $H = 40$ nm, $W = 100$ nm, $D = 40$ nm. The black line shows the propagation length of the gap mode.

the reduction of the plasmonic decay rates and SE β-factor, the dielectric inhomogeneity also decreases the propagation lengths by a factor of 5 compared with the homogenous case, which might make the out coupling of the optical plasmons challenging.

Moreover, as can be seen from Fig. 4, the plasmonic decay rate and SE β-factor are rather sensitive to the gap width (D), but not to the height of the metals (H). The interpretation is that the transverse mode profile of the gap mode is mainly determined by the gap-width, rather than the height of the metal. Therefore we take the height H as a fixed value ($H = 40$ nm), and examine the position as well as the gap width dependence of the plasmonic decay rate and SE β-factor, cf. Fig. 5. As can be seen from Fig. 5, the plasmonic decay rate and the SE β-factor increase when the gap width becomes smaller, which originates from the stronger confinement of the field for the waveguide with smaller gap width. Regarding the position dependence, the plasmonic decay rate drops when the emitter is moved away from the metals, while the SE β-factor remains almost the same when Y_{QDs} is smaller than 50 nm. We also observe that the maximum SE β-factor (close to 60%) is achieved at a position outside the gap for $D = 20$ nm. Another striking difference between the homogenous dielectric environment [9] and the inhomogenous dielectric environment with the same geometric sizes is that the SE β-factor is reduced significantly. The leaky modes that appear due to the inhomogeneity of the waveguide [14], and are confined in the coating region and leak away through the substrate region, thus seriously impact the achievable SE β-factor.

Our interpretation in terms of the significant role played by the leaky plasmonic modes is confirmed by the inhomogeneity dependence study in Fig. 6. An increased value of n_c, has three consequences: (I) The field will distribute more homogenously, which results in an increase of the plasmonic decay rate, especially for the emitter positioned in the middle of the

gap; (II) The leaky plasmonic modes will contribute less, and we also observe that the SE β-factor is increased to above 50%. As can be seen from Fig. 3, decreasing the index contrast of the dielectric environment will narrow the spectal range of leaky plasmonic modes, and consequently their contributions will be suppressed; (III) The propagation length becomes shorter since the increased value of n_c will give rise to a larger value of the effective mode index, consequently the mode will become more confined. When increasing n_c beyond the value of 2, higher order modes will be excited for the particular waveguide in Fig. 6, the study of which is outside the scope of the present paper.

4. Conclusion

In conclusion, we studied the efficiency with which emission from a single self-assembled quantum dot can be coupled to a realistic metallic slot waveguide. With typical structure sizes, the emitted radiation can be efficiently coupled to a single guided mode supported by the metallic slot waveguides. We find that the SE β-factor for the excited mode depends strongly on the parameters of the waveguide, especially on the homogeneity of the surrounding structure. Compared to the case of coupling to a metallic slot waveguide with symmetric dielectric environment, the SE β-factor is strongly reduced. We attribute the significant reduction to the leaky modes induced by the inhomogeneity. By increasing the refractive index of the coating layer to minimize the impact of the leaky plasmonic modes, we found that the coupling efficiency of the quantum dot to the single mode supported by the metallic slot waveguide can be above 50%. We also found that there is a balance between the coupling efficiency and the propagation length of the optical plasmons, which indicates that in addition to the competition between the three channels of spontaneous emission decay, the propagation loss of the optical plasmons needs to be taken into account, to achieve a high overall efficiency of a plasmon-based single-photon source.